

AVO ANALYSES AND SPECTRAL DECOMPOSITION OF SEISMIC DATA, OFFSHORE NILE DELTA, EGYPT

S.E. Mahmoud⁽¹⁾, K.S. Ahmed⁽¹⁾ and M. Radwan⁽²⁾

(1) Geophysics Department, Faculty of Science, Cairo University, Giza, Egypt.

(2) BG Egypt.

خواص الآفو والتحليل الطيفي للمعطيات السيزمية في المنطقة البحرية لدلتا النيل في مصر

الخلاصة: يركز هذا البحث بالأساس على دراسة بئرين من العصر البليوسيني تقعان في الجزء الشرقي من منطقة امتياز غرب الدلتا البحرية لإثبات أن الاستخدام المناسب للتحليل AVO يشكل أداة قيمة للاستكشاف. لقد اختبرت هاتان البئران خزانات بها نسبة غاز ضئيلة وأثبتت الدراسة أنهما مختلفان في خواص AVO والتحليل الطيفي.

و يعد فهم تأثير الغاز على خواص الخزان و تصنيفات AVO في البئرين أحد الأهداف الرئيسة لعمل هذه الدراسة. ولقد أظهرت نتائج التحليل الطيفي على خواص الخزان في البئرين أن السلوك معقد الى حد ما في البئر "أ" و أن البئر "ب" تظهر سلوكاً منظماً في الترددات المختلفة.

ABSTRACT: This paper principally focuses on the analysis of two Pliocene wells located in the eastern part of the West Delta Deep Marine concession, Offshore Nile Delta demonstrates that the appropriate use of AVO analysis forms a worthwhile and valuable tool for exploration. These wells encountered low gas saturation reservoirs and this study indicates that they are different in both the AVO behavior and their spectral characteristics.

One of the primary aims of performing AVO analysis is to provide an improved understanding of AVO classifications of the encountered reservoirs, and the way to differentiate fluid effects from lithology in the Pliocene strata. For this study, there is a special focus on the examination of the offset stack data and the AVO cross plot analysis. For well (B), Class III AVO anomaly is consistent with theoretical predictions for frequency-dependent AVO behaviors. Results from the spectral analysis of well(A) show rather complicated behavior in the iso-frequency sections that cannot be fully explained. Generally, the amplitude anomalies for both wells were originally interpreted to be quite similar but this study indicates they are different in both the AVO behavior and their spectral characteristics.

Spectral decomposition is applied to full stack seismic data covers these wells and provides further evidence for some differences in the spectral behavior of the reservoirs at both wells.

Geological Setting

The study area is a subset of the West Delta Deep Marine (WDDM) 3D Seismic, Offshore Nile Delta, Egypt. The Two wells were used are in the deep water (250-1500m) of Nile Delta Figure (1).

The Nile Delta basin, as a part of the regional Eastern Mediterranean basin, has been affected by the complex evolution of the regional as a result of African, Eurasian and Arabian inter plate movements. This has reached its climax during the Miocene with the opening of the Gulf of Suez – Red Sea rift.

The structural architecture of the Nile Delta offshore is mainly shaped by the interplay, intersection and linking of main fault trends. These are the Northeast-Southwest trending Rosetta fault; Northwest – Southeast oriented Tensah fault; East – West trending faults and NNW – SSE trending faults (Baltim / Abu Madi) (Aal et al., 2000).

The Nile Delta basin is bounded to the south by an E – W trending hinge zone, that plays an important role in the stratigraphic and tectonic evolution (Said 1981). This structural belt, active in different stages since the Jurassic, represents the boundary between the southern stable platform (South Delta block) and northern. This hinge line became active during the Oligocene. Basinal province and resulted in dramatic thickening of the Oligocene and Miocene sediments to the north.

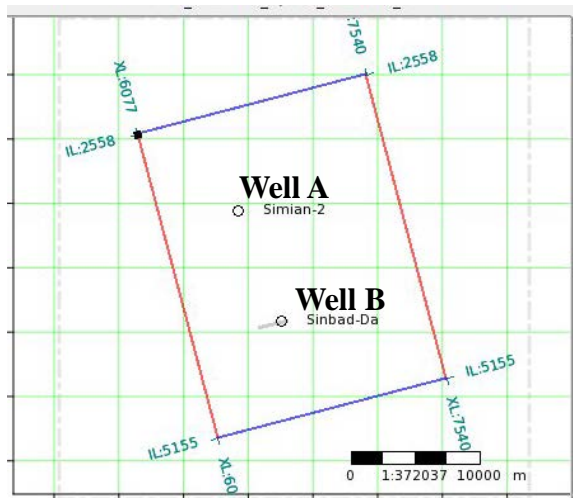


Figure 1: Location map of wells (A & B).

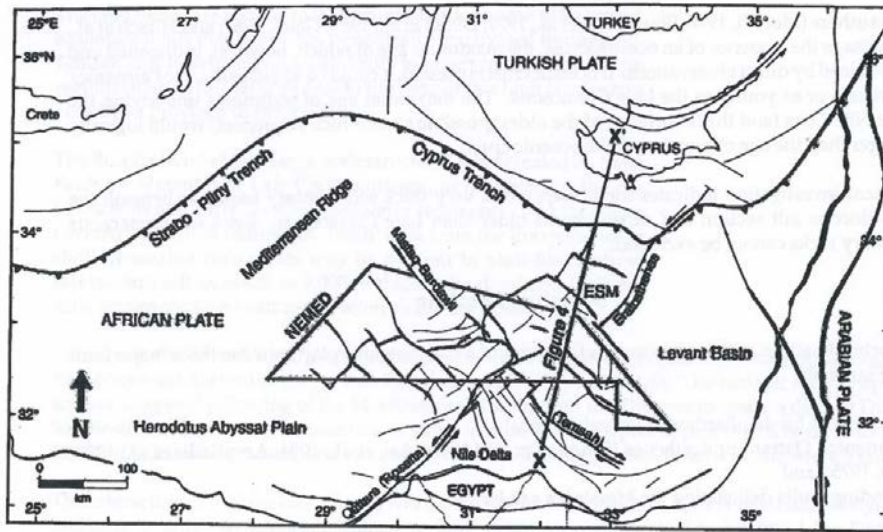


Figure 2: Tectonic setting of the Mediterranean Basin. (from Aal et al, 2001).

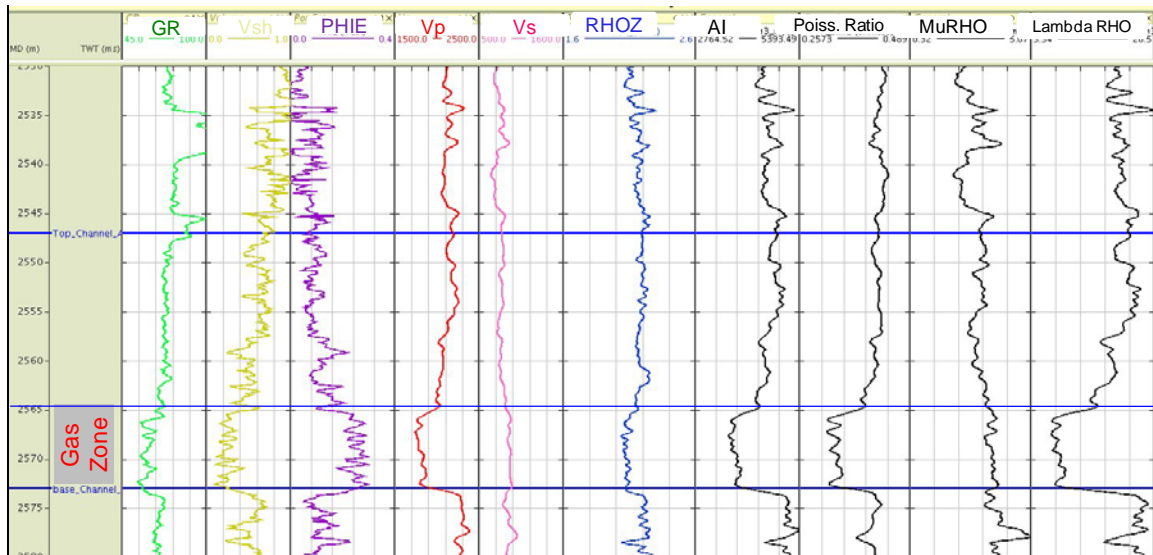


Figure 3: Well A Logs and calculated elastic logs (AI, PR, MuRHO and Lambda RHO) which are decreasing within the gas reservoir.

The NE – SW Rosetta fault trend is possibly related to Cretaceous structures, that continued to have a strong impact on the younger Tertiary sequences. It shows compressional and extensional regimes operating in space and time. The old compressional regime represented by inversion and thrusting tectonics, younger whereas extensional is represented by normal faulting (Sehim et. al 2002).

The NNW – SSE Baltim / Abu Madi Structural trend is formed by the reactivation of the older pre-Tertiary structure during early Miocene. These faults occasionally cut the Messinian unconformity and continue into the Pliocene sequence.

The West Nile Delta sub-basin is a proven hydrocarbon province, with significant discoveries of gas, condensate and oil. The Tertiary section has all the components of petroleum system, reservoirs, seals and

source rocks in (Oligocene – Miocene (thermogenic) and Pliocene (biogenic)).

I) Rock physics Analysis:

The Rock physics study was useful in understanding how reservoir properties affect seismic response and aids interpretation. Additionally, such a study was essential in determining which if any geophysical methods are applicable for the enhanced delineation of such reservoir properties, for example inversion and AVO.

The work has produced depth trends for compressional-wave velocity, density and acoustic impedance as well as relationships between reservoir parameters, such as porosity, and acoustic properties as shown from the figures below. The effective porosity of the reservoir of the Well (B) is a little bit higher than well (A) figures(3&4).

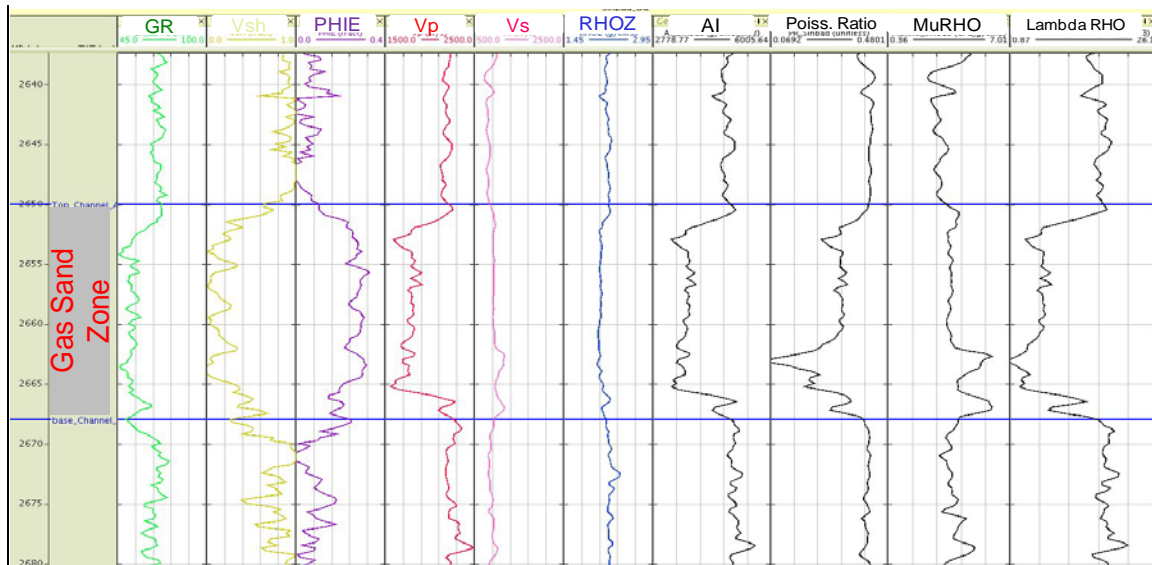


Figure 4: Well B Logs and calculated elastic logs (AI, PR, MuRHO and Lambda RHO) which are decreasing within the gas reservoir.

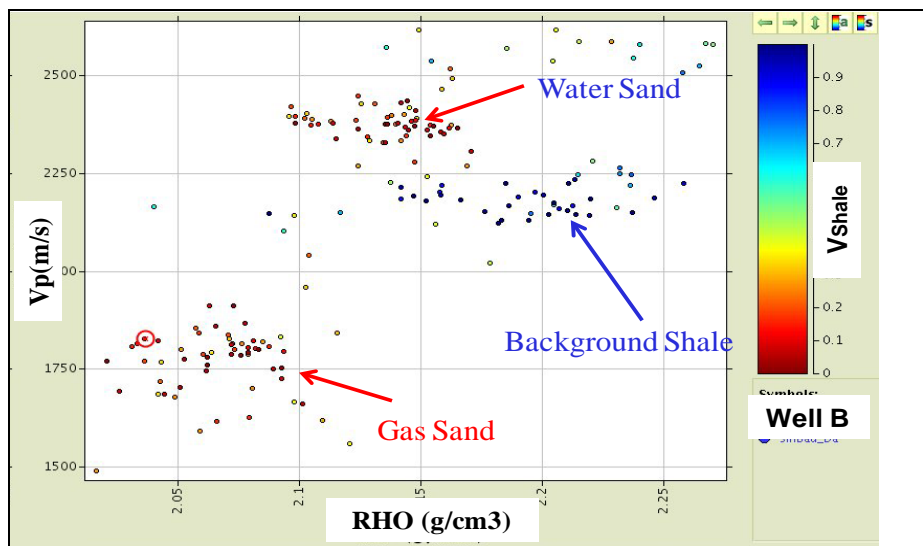


Figure 5: Vp-density cross plot showing a good separation between the gas sand, water sand and the back ground shale. Red points represent sands; blue points represent shale and colour coded by Vsh.

It is noticed $\lambda\rho$ is changed a lot between the gas reservoir and the background shale at both wells as it is sensitive to the fluid type and the $\mu\rho$ is sensitive to the rock matrix figure (3&4).

Figure (5) shows a clear decrease in compressional velocity (Vp) of the gas sand reservoir if it is compared to the brine sand and the background shale. This is the general Pliocene Rock physics model within the Nile Delta.

The seismic response of any reservoir is governed by the properties of both the reservoir itself and those of the encasing media and it was clear from the different properties Cross-plots that the gas sand has a lower acoustic impedance than the background shale at the reservoir intervals of both wells figure (6).

Single interface Blocky AVO modelling has been generated .AVO Intercept – gradient probability functions have been generated by calculating the AVO response for these interface models comprising shale over sand. The properties (Vp, Vs and density) for these models were taken from individual log samples classified as representing brine sand, hydrocarbon-bearing sand and shale according to the clay volume and water saturation curves. This approach provides a realistic estimation of the range of responses which may be expected. It should be noted, however, that this kind of modelling does not take into account the effect of the seismic wavelet and often produces optimistic results. The cross plots of Sin2θ VS reflection coefficient were generated.

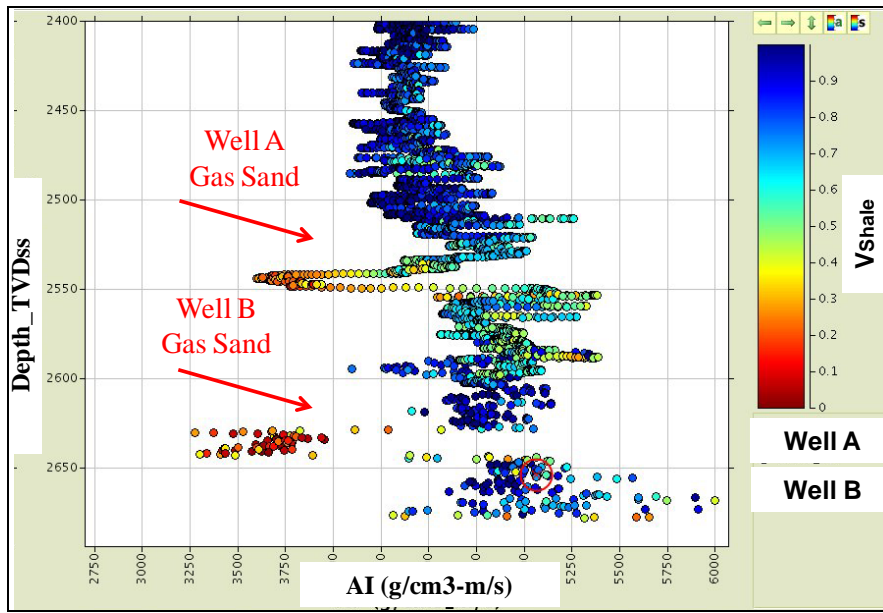
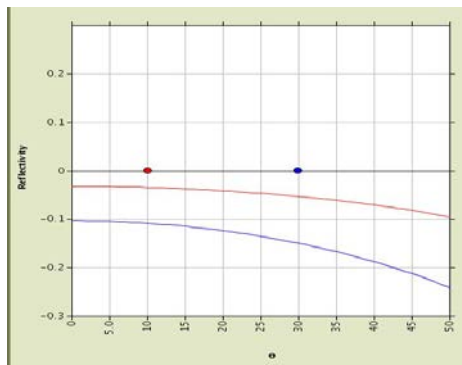
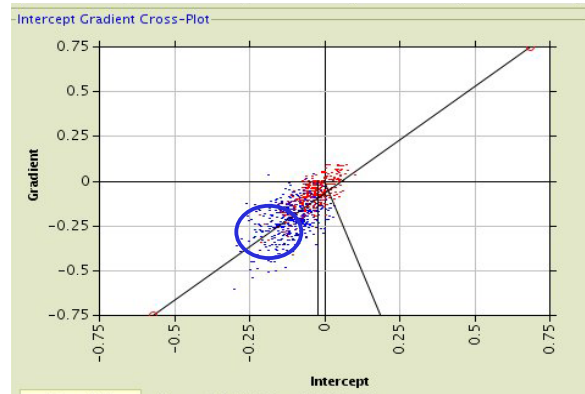


Figure 6: AI Depth trend for both wells A and B. The gas sand reservoirs have a lower AI trend than the background shale.



— Well A : Shale above Gas Sand
 — Well B : Shale above Gas Sand



● Near
 ● Far

Intercept Gradient Values										
Display	Colour		I	G	Class I	Class IIp	Class II	Class III	Class IV	Class FC
<input checked="" type="checkbox"/>	Red	Well A : Shale above Gas Sand	-0.03	-0.085	0.092	0.068	0.142	0.562	0.015	0.12
<input checked="" type="checkbox"/>	Blue	Well B : Shale above Gas Sand	-0.107	-0.223	0.005	0.035	0.042	0.91	0.008	0

Figure 7: AVO Blocky models for both Wells .Well (B) shows a clear Class III AVO response while well (A) doesn't show a clear AVO response.

II) Comparison of AVO analyses from two wells:

AVO analysis is increasingly becoming part of the everyday workflow; however it is often found that existing data sets require further conditioning in order to extract accurate reservoir properties within the zones of interest.

The Trim Statics process was applied to fix migration move-out problems on pre-stack data. With this process we adjust the time an event occurs by controlled parameters. The output results were QC'd to make sure the stretching is not affecting other events as shown in figure (8).

To carry out the AVO analysis, stack data of near, middle and far offsets were used to check the relative amplitude variations in each offset range. For well(B), Class III AVO can typically be seen and a more complicated AVO response for Well (A). common cross-plot of AVO intercept and gradient attributes help to separate the lithology and fluid responses from the background trend. By combining intercept and gradient stacks along an angle of rotation, fluid and lithology stacks can be produced. The key parameter to generate the fluid and lithology stacks is the fluid angle. This angle is typically defined by the apparent Vp/Vs ratio of the background or shale trend on the cross-plot.

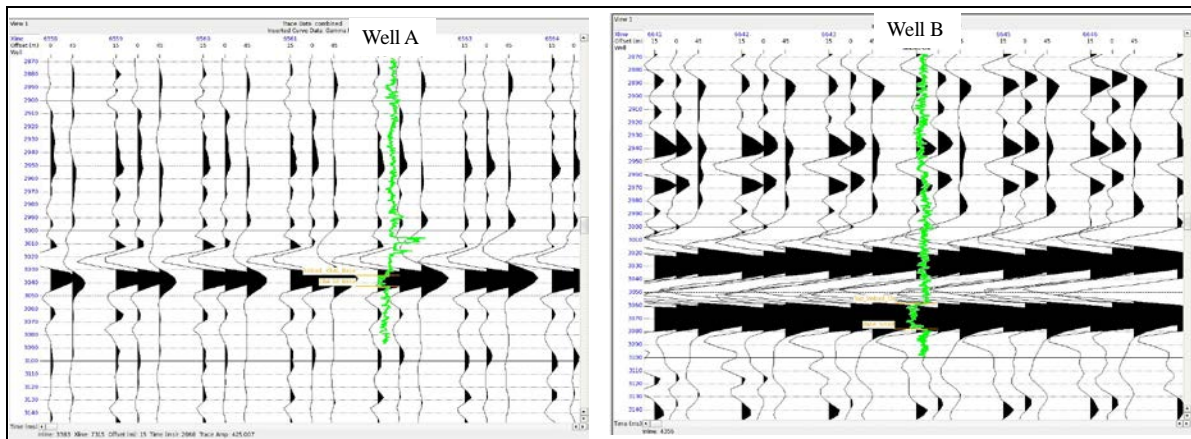


Figure 8: Condition the angle stacks using trim static.

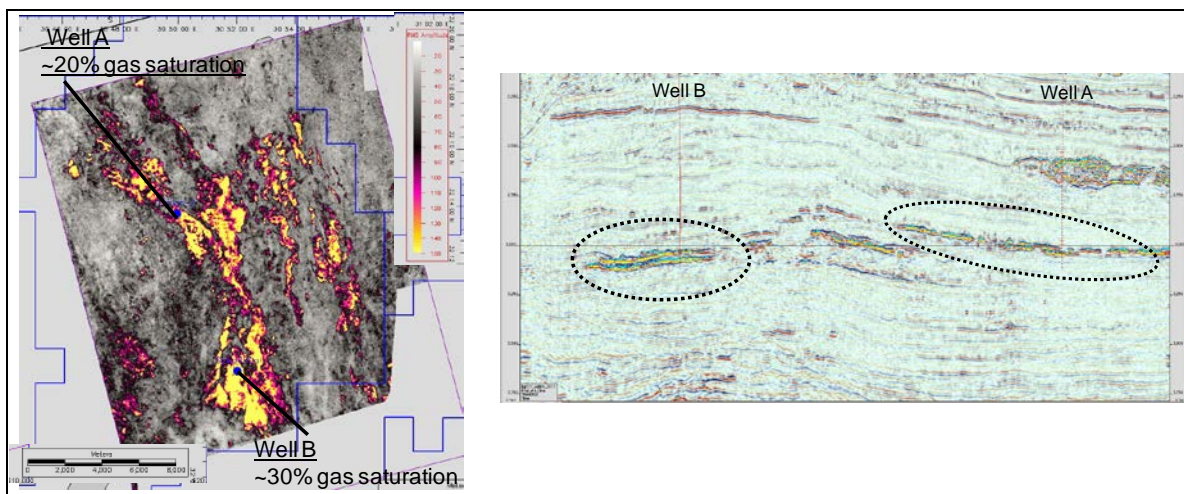


Figure 9: Wells (A) and (B) positioned on a high amplitude anomaly.

AVO attributes extracted from well logs can be different from seismically-extracted attributes because of the offset-dependent tuning and NMO stretch, selected angle range and the approximations in the equations.

Figure (9) shows that the two wells tested a very bright amplitude anomaly on the full offset stack.

The angle stacks shows an increase in the amplitude with angle at the reservoir level of Well B and a less pronounced increase in the amplitude with offset at the reservoir level of Well A as shown in Figure 10.

The figures below show some AVO attributes on the reservoir levels of the two wells. The top reservoir is represented by a soft kick (decrease in the AI) and the base reservoir is a hard kick as shown from the stacks data.

III) Spectral decomposition analysis:

Spectral decomposition is an ideal tool to detect the effect of frequency-dependent AVO. There are a variety of spectral decomposition methods. These include the DFT (discrete Fourier Transform), MEM (maximum entropy method), CWT (continuous wavelet transform), and MPD (matching pursuit decomposition). Each method has its own advantages and disadvantages, and different applications require different methods.

To perform the spectral decomposition and spectral analysis, we used short-window Fourier transform which is the classical way to extract and evaluate frequency spectrum of data in seismic data processing, when experts interested in data from a long window. To concentrate on the target area (e.g. a faulted horizon slice) we need decreasing the window length, the frequency resolution in frequency domain will be compromised.

The use of frequency decomposition colour blending has become commonplace in the analysis of stratigraphic formations from 3D seismic data (Partyka et al., 1999; Henderson et al., 2007, 2008). Red-green-blue (RGB) colour blending is a particularly effective way of displaying multiple frequency decomposition responses. The interference between different frequency bands can reveal startling detail within the colour blend, and can highlight very subtle features of sub-seismic resolution. Detailed analyses of spectral characteristics have revealed that Classes II and III show different responses to fluid saturation at low and high frequencies (for an example of spectral decomposition for Class I AVO, see Chapman et al. 2005, 2006).

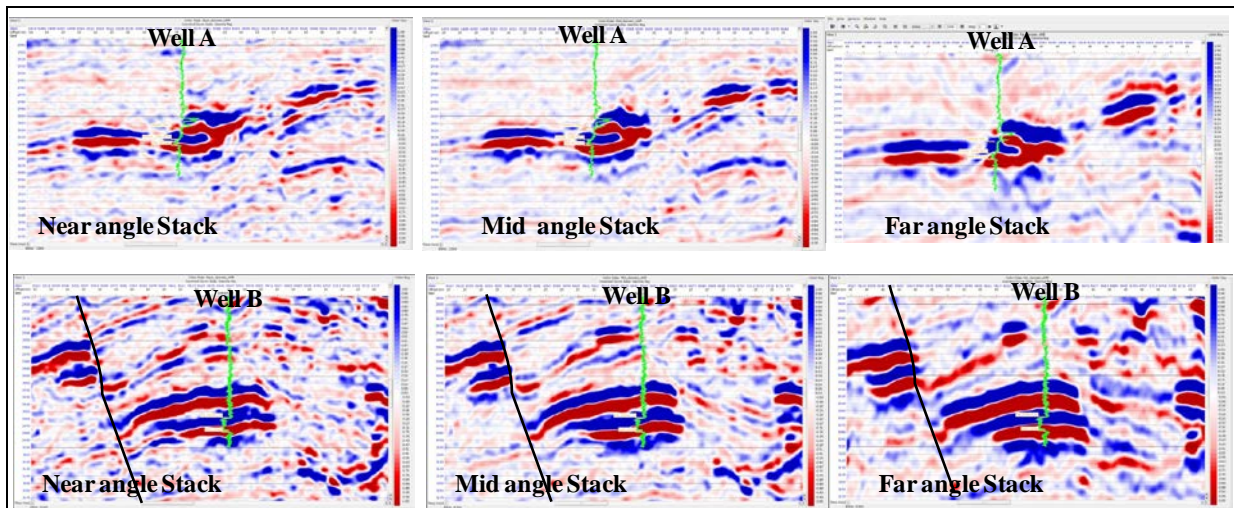


Figure 10: Different angle stacks through both Wells (A) and (B).

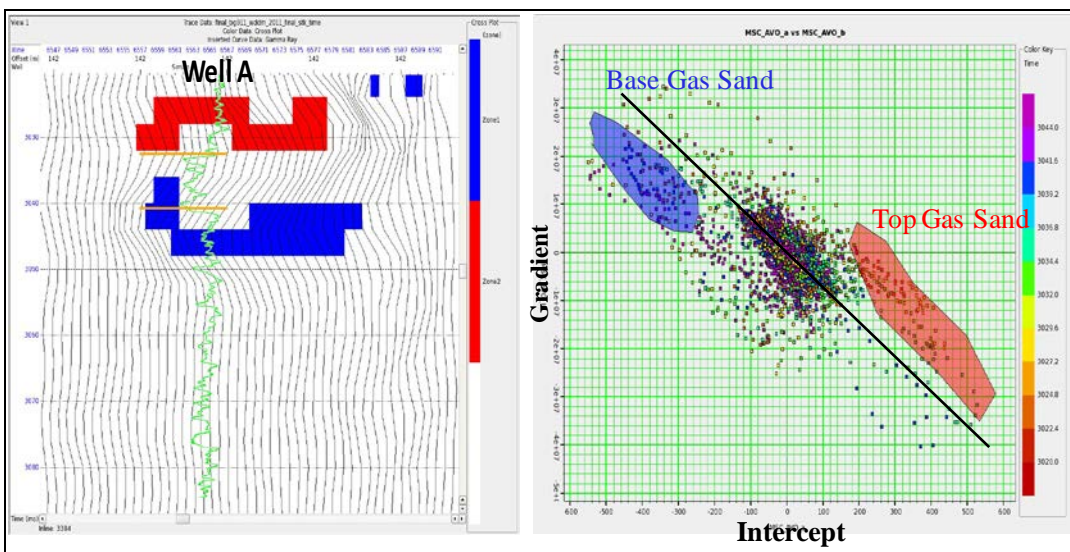
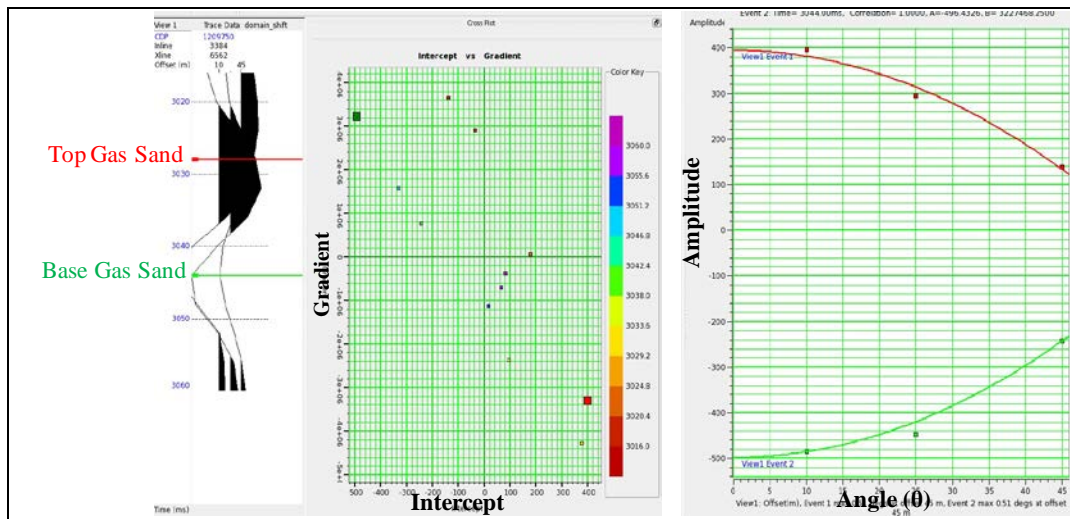


Figure 11: AVO cross-plot for well (A) shows a complicated AVO response. Top gas sand is a soft peak (decrease in AI).

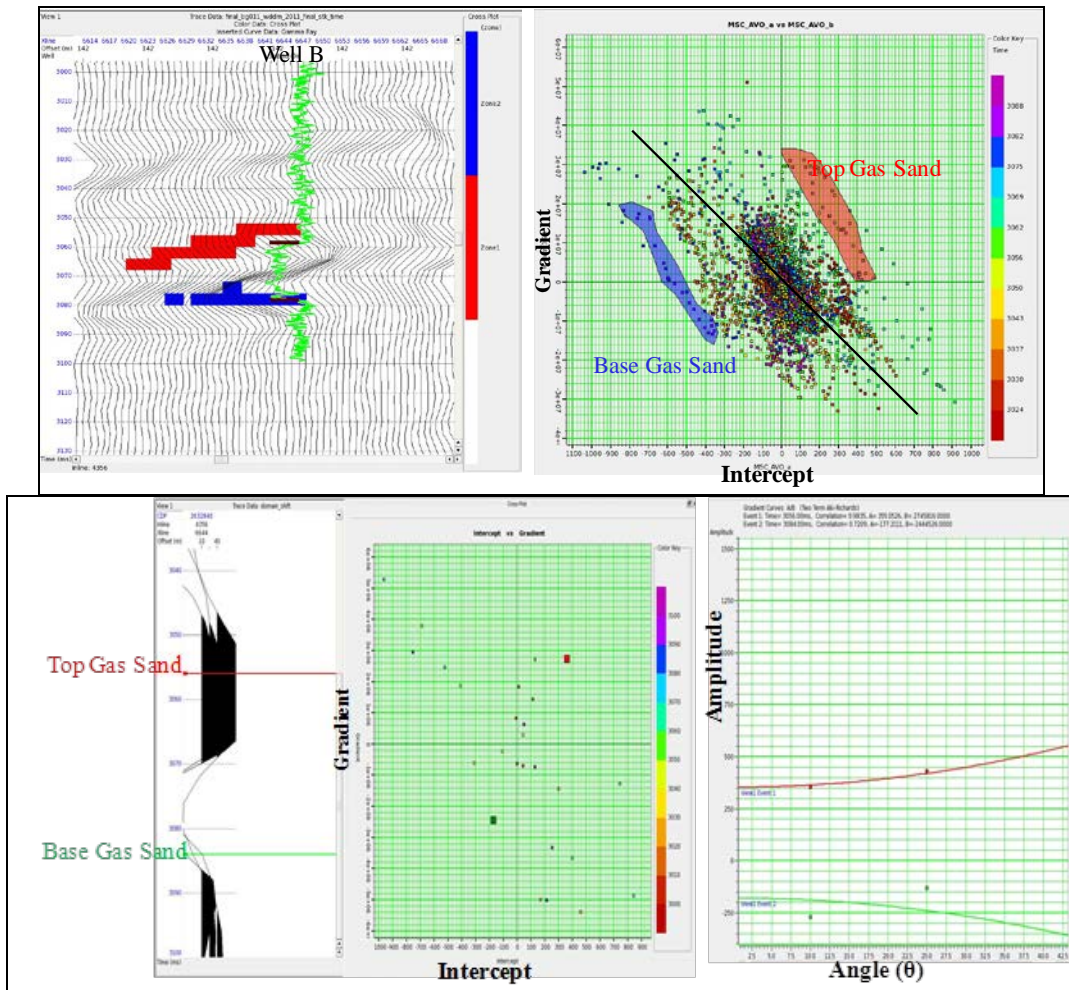


Figure 12: AVO cross-plot for well (B) shows a class III AVO response. Top gas sand is a soft peak (decrease in AI).

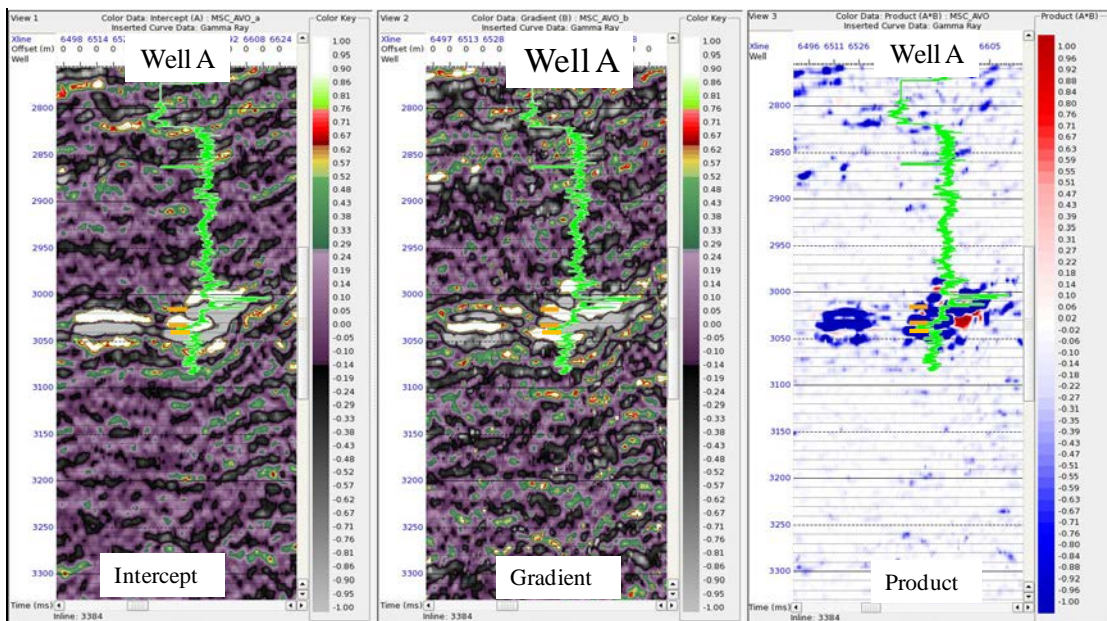


Figure 13: The AVO product shows a negative response at the top and base of the clastic reservoir.

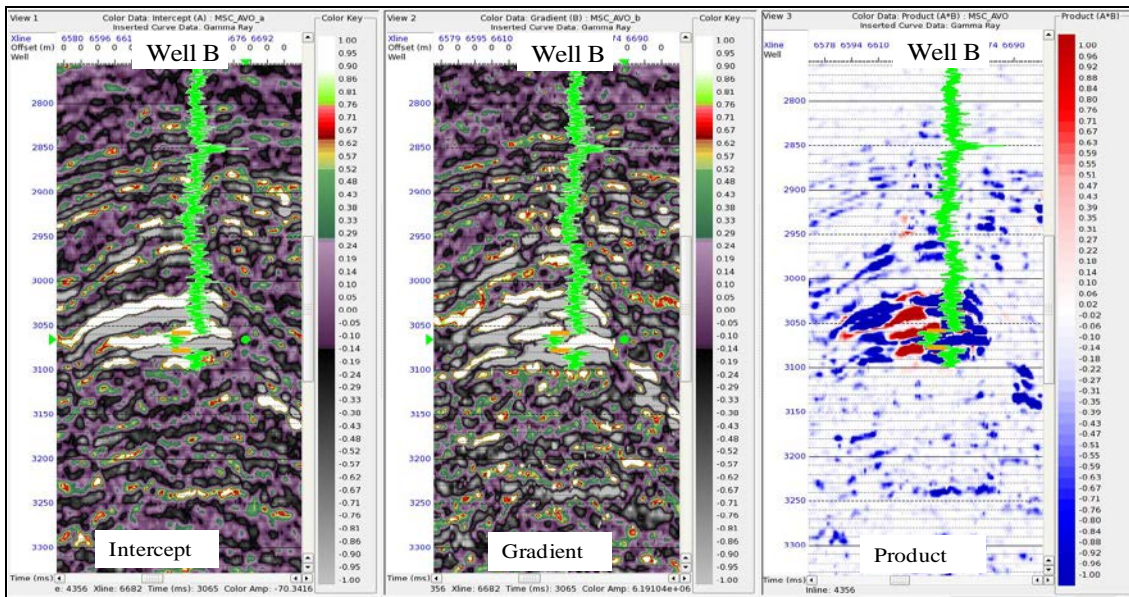


Figure 14: The AVO product shows a positive response at the top and base of the clastic reservoir, which can indicate the presence of hydrocarbons. This attribute works well for a class 3 AVO response.

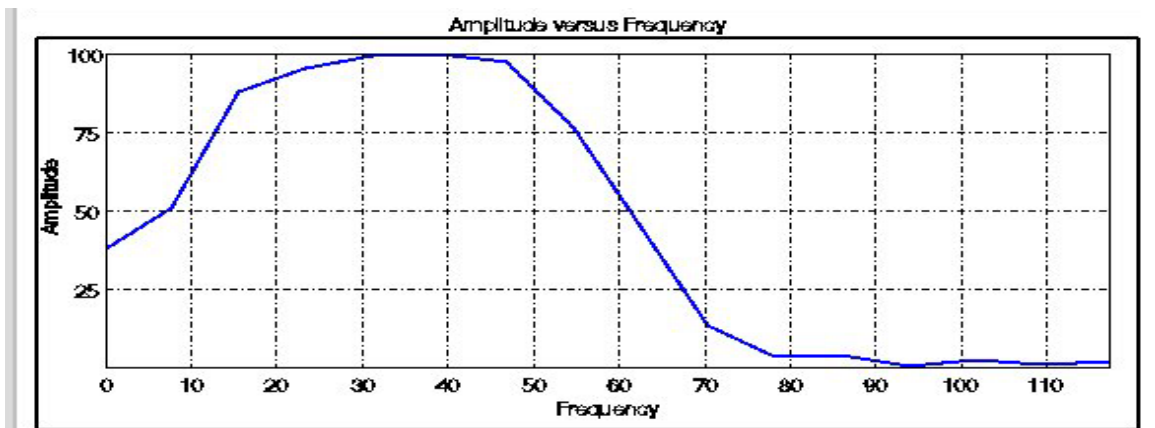


Figure 15: Amplitude spectrum for the Full stack seismic calculated within the interval (2600-3400 ms). The dominant frequency is about 35 Hz at that level

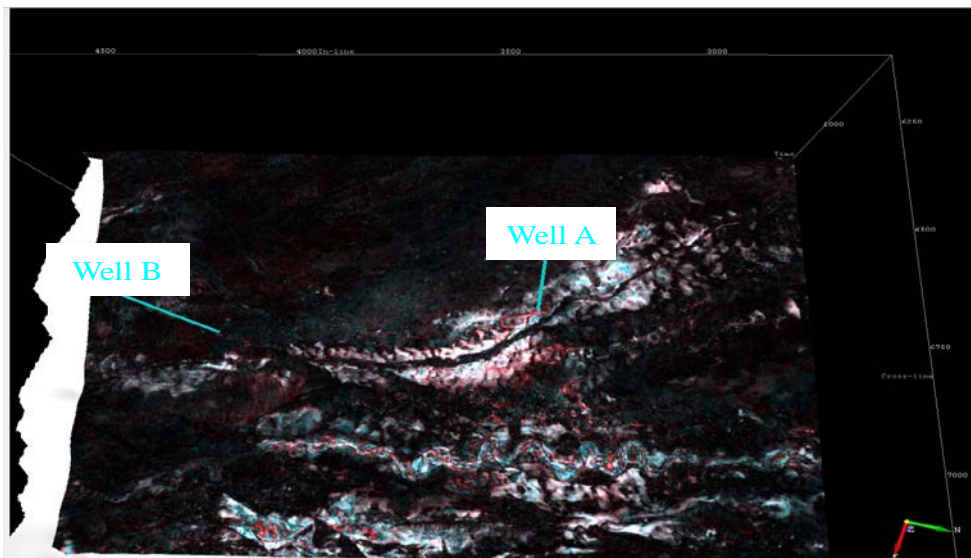


Figure 16: A colour blended map view of the spectral decomposition (red- 25 Hz, green-30Hz, blue- 35 Hz) on the top Well (A) reservoir. It shows that the well isn't in properly testing this level.

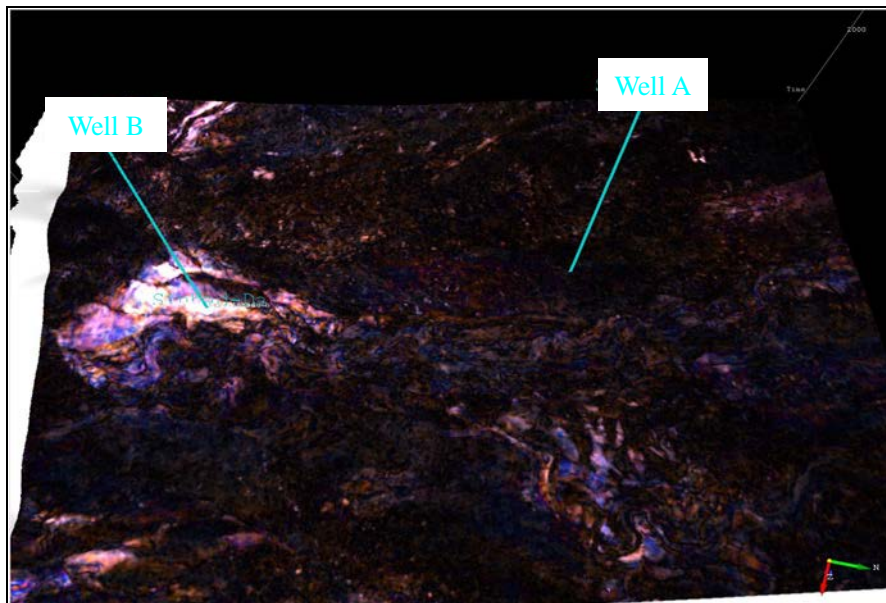


Figure 17: A colour blended map view of the spectral decomposition (red- 25 Hz, green-30Hz, blue- 35 Hz) on the top Well (B) reservoir. It shows that the well drilled bright anomaly towards the down dip.

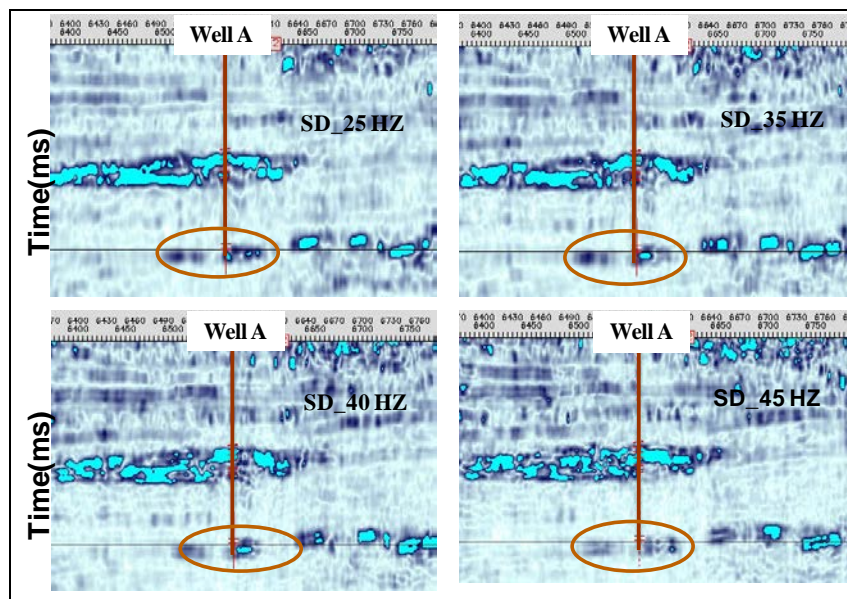


Figure 18: Selected iso-frequency sections of the stacked seismic data. We can observe that the amplitudes in the marked area change markedly from an increase with frequency between 35 Hz and 40 Hz, to a decrease with frequency at 25 Hz. This suggests that this anomaly is indeed concentrated on the very a moderate frequency range over a very narrow frequency band. The increase of amplitudes with frequency is consistent with the prediction but the sudden decrease thereafter cannot be fully explained.

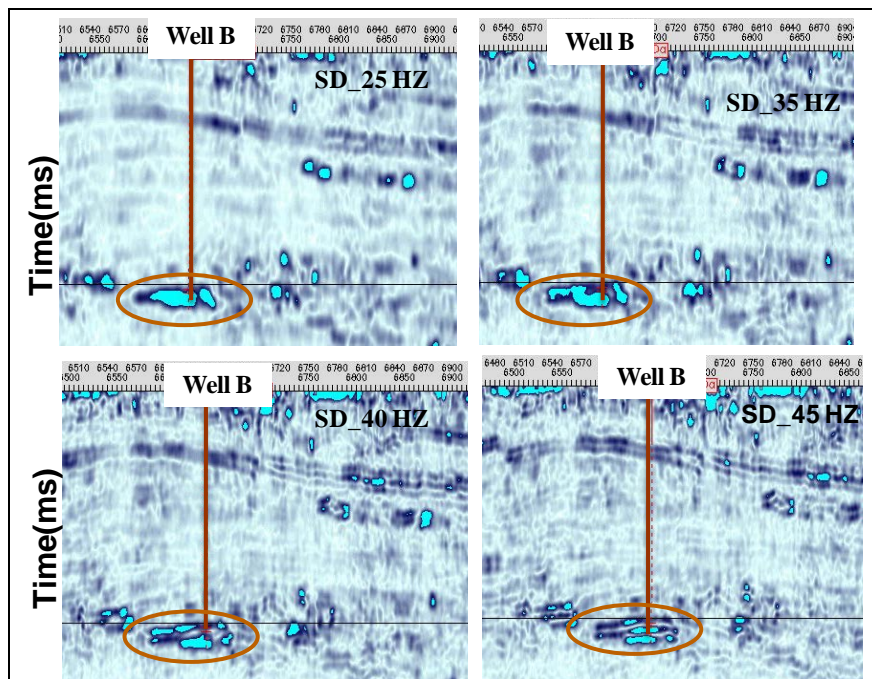


Figure 19: Selected iso-frequency sections of the stacked seismic. We can see a systematic decrease of amplitudes with frequency in the marked target areas which is qualitatively consistent with the prediction for the Class III AVO. The vertical axis is two-way travel time in seconds.

In particular, it is suggested that the changes in AVO signatures for Well A and B are more likely related to the fluid saturation. Spectral analyses also reveal the strong effects caused by tuning (when wavelength is comparable to, or greater than, the layer thickness) as shown by Partyka et al. (1999) and recently demonstrated by Chapman et al. (2006). The study has focused on the evaluation of two wells with associated seismic datasets all of which have amplitude-related anomalies. Not surprisingly, the two wells have different characteristics in terms of AVO signature.

CONCLUSION

The Well (A) gas reservoir shows a clear Class III AVO response from the blocky models generated from logs and also the AVO attributes from angle stacks. The spectral decomposition results reveal that there are some differences in the spectral characteristics of the gas reservoirs at the two wells. Well (B) gas reservoir shows a clear and consistent behaviour with the frequency while well (A) gas reservoir shows rather complicated behaviour in iso-frequency sections that may indicate different effect of the gas saturations.

ACKNOWLEDGEMENTS

Authors would like to thank BG Egypt for providing the required data required to carry out this study. We would also like to express great thanks to the Thibaut Cheret from BG Egypt for his guidance and continuous support.

REFERENCES

- Batzle, M.L., Han, D.H. & Hofmann, R. 2006.** Fluid mobility and frequency dependent seismic velocity – direct measurements. *Geophysics*, 71, N1-N10.
- Castagna, J.P. & Smith, S.W. 1994.** Comparison of AVO indicators: A modeling study. *Geophysics*, 59, 1849-1855.
- Castagna, J.P., Sun, S. & Siegfried, R.W. 2003.** Instantaneous spectral analysis: detection of low frequency shadows associated with hydrocarbons. *The Leading Edge*, 22, 127-129.
- Castagna, J.P., Swan, H.W. & Foster, D.J. 1998.** Framework for AVO gradient and intercept interpretation. *Geophysics*, 63, 948-956.
- Partyka, G.J., Gridley, J. & Lopez, J. 1999.** Interpretational application of spectral decomposition in reservoir characterization. *The Leading Edge*, 18, 353-360.